Polarization waves in dielectric films with spatial dispersion

2002 J. Phys.: Condens. Matter 14 1745

(http://iopscience.iop.org/0953-8984/14/8/305)

INSTITUTE OF PHYSICS PUBLISHING JOURNAL OF PHYSICS: CONDENSED MATTER

J. Phys.: Condens. Matter **14** (2002) 1745–1763 PII: S0953-8984(02)30343-6

Polarization waves in dielectric films with spatial dispersion

Jean-Pierre Jardin[1], **Philippe Moch**[1] **and Vladimír Dvorák**[2]

[1] Laboratoire des Propriétés Mécaniques et Thermodynamiques des Matériaux, CNRS, Institut Galilée, Université Paris-Nord, Avenue J-B Clément, 93430 Villetaneuse, France
[2] Institute of Physics, Academy of Sciences of the Czech Republic, Na Slovance 2, 182 21 Prague 8, Czech Republic

E-mail: moch@lpmtm.univ-paris13.fr and pmoch@club-internet.fr

Received 1 November 2001
Published 15 February 2002
Online at stacks.iop.org/JPhysCM/14/1745

Abstract
The polarization waves propagating in a slab-shaped or in a semi-infinite dielectric medium with spatial dispersion characterized by a volume free-energy density and by a boundary-surface energy density are studied, taking into account Maxwell's equations, in the framework of the Landau–Ginzburg formalism. It is shown that two independent extrapolation lengths providing for the required additional boundary conditions need to be specified at each surface limiting the medium. Complete calculations are performed in the electrostatic approximation: they provide evidence of the differences between the transverse in-plane polarized modes (s modes) and the sagittal plane polarized modes (p modes). True surface modes exist only in the case of negative extrapolation lengths. A detailed analysis of the symmetry properties of the surface and of the guided bulk modes in a slab is developed. Finally, our results are compared with those from previous models describing the boundary conditions in media where spatial dispersion is present.

(Some figures in this article are in colour only in the electronic version)

1. Introduction

The problem of normal modes of vibration in an ionic crystal slab has a long history but it is still of some concern because of the general interest in the properties of thin films of various materials. In particular, ferroelectric films have been intensively studied both experimentally and theoretically (see [1] for example, and references therein) because of their device applications. So far, the problem of normal modes has been solved for a semi-infinite ferroelectric only and, as we shall explain later, not completely. It is the aim of this paper to solve the problem for a slab using the language of Landau theory of phase transitions, to point out some shortcomings of theories previously elaborated for a semi-infinite ferroelectric

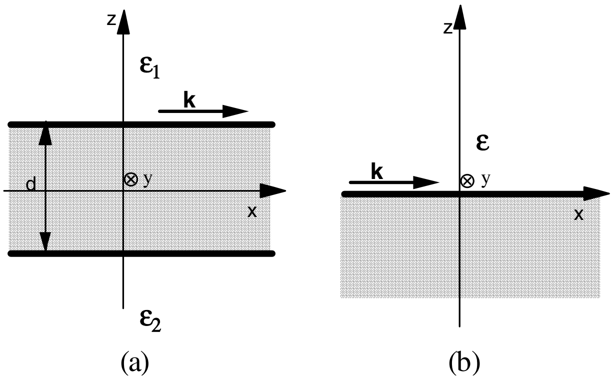

Figure 1. Schematic diagrams of the systems studied: (a) a dielectric slab; (b) a semi-infinite dielectric medium.

and to discuss the results in the context of what has already been done for a slab made of an ordinary ionic crystal. Our model generally relates to dielectric materials showing spatial dispersion. In principle, it can be used to describe polarization waves in the paraelectric phase of ferroelectric films about which experimental information concerning the surface properties is continuously growing. A further generalization could involve the ferroelectric phase.

Our procedure will be purely phenomenological (as is common with ferroelectrics)—that is to say, we shall consider long-wavelength optical modes only, which will be treated as modes of the macroscopic polarization $\boldsymbol{P}$. We shall consider a slab of thickness d (perpendicular to the z-axis), infinite in the x- and y-directions, and polarization modes propagating in a direction parallel to the planes of the slab (figure 1). Because of the translation symmetry in the (x, y) planes, polarization waves are wavelike, i.e. polarization waves are characterized by the two-dimensional wavevector $\boldsymbol{k}(k_x, k_y)$ which should satisfy $ka \ll 1$ in order to make a macroscopic description possible (a denotes the lattice constant).

The problem to be solved is that of how the angular frequencies ω of polarization waves depend on k and how the amplitudes of these waves vary in the direction perpendicular to the film, i.e. along the z-axis. We begin by formulating the problem in general, i.e. including the retardation of fields, but solutions will be sought for in the electrostatic approximation, neglecting the interaction of the polarization waves with the transverse electromagnetic field of free photons. In other words, we shall not discuss polaritons, and will limit ourselves to waves with wavevector in the range $\omega/c \ll k \ll a^{-1}$. It is well known [2] that in general two types of mode exist in this case:

(1) *Bulk modes (BM)* (sometimes called guided—by the surfaces of the film—modes). The variation of their amplitudes across the film is sinusoidal in character,
(2) *Surface modes (SM)*. Their amplitudes decrease exponentially with increasing distance into the film from the surfaces.

It should be pointed out that when the slab is surrounded by the same medium on both sides and if we take the origin of the coordinate system in the middle of the slab, then the plane $z = 0$ is the symmetry plane of the problem. Consequently, the components P_i of the normal modes should be either even or odd with respect to change of z into $-z$.

Let us now briefly recall how the normal modes of a slab are found in a macroscopic theory using the so-called permittivity formalism [2]. Maxwell's equations (in the electrostatic approximation) completed by the material relation between the displacement vector $\boldsymbol{D}$ and the electric field $\boldsymbol{E}$, are solved under appropriate boundary conditions, i.e. D_z and $E_{x,y}$ should be continuous on the slab surfaces. Two qualitatively different situations should be distinguished: the crystal of which the slab is made is spatially dispersive (i.e. the relation between $\boldsymbol{D}$ and $\boldsymbol{E}$ is non-local) or it is not. The origin of this qualitative difference is that, without spatial dispersion, Maxwell's equations, the continuity of $E_{x,y}$ and D_z at the surfaces and the permittivity $\varepsilon(\omega)$ determine normal modes of the slab unambiguously [3, 4]. If, however, the spatial dispersion of $\varepsilon(\omega)$ is taken into account, additional boundary conditions (ABC) are needed for solving the problem [5]. We shall return to this point later. Without the spatial dispersion, $\varepsilon(\omega)$ depends on the frequency only and not on the wavevector. The permittivity of the slab is taken as the same as that of an infinite (in all three dimensions) crystal (for simplicity we consider a crystal of cubic symmetry, for which $\varepsilon_{ik} = \varepsilon\delta_{ik}$)—that is, in the form

$$\varepsilon(\omega) = \varepsilon_\infty \frac{\omega_\mathrm{l}^2 - \mathrm{i}\omega\gamma - \omega^2}{\omega_\mathrm{t}^2 - \mathrm{i}\omega\gamma - \omega^2} \tag{1}$$

where ω_l and ω_t are the frequencies of the bulk longitudinal and transverse modes, respectively (ε_∞ stands for the background permittivity at $\omega \gg \omega_\mathrm{t}$ and γ is the damping constant). Let us choose the direction of $\boldsymbol{k}$ along the x-axis: $\boldsymbol{k}(k, 0)$. Then it follows from Maxwell's equations that P_y-waves (s polarization) are decoupled from the system of coupled P_x- and P_z-waves (p polarization). Obviously, the P_y-waves produce neither volume nor surface electrical charges, and consequently $\boldsymbol{E}$ is equal to zero everywhere. Hence the corresponding BM have the frequency ω_t [2]. Furthermore, there are no SM in this case.

Let us now turn to p-polarized waves: in addition to two series of BM at frequencies ω_l and ω_t, two SM occur [3]. In the case of symmetrical surroundings, the first SM, of lower frequency, has an even P_x-component and an odd P_z-component, and vice versa for the second SM. The frequencies of these SM lie between ω_t and ω_l, and in the limit $kd \gg 1$ they become practically degenerate. When $k \to 0$ both SM cease to be localized near the surfaces and, at $k = 0$, P_z- and P_x-waves are completely decoupled: one mode becomes a pure P_z-wave with a constant amplitude across the slab and a frequency ω_l; the other mode changes into a pure P_x-wave with a constant amplitude and a frequency ω_t. The disappearance of SM at $k = 0$ is a shortcoming of the permittivity formalism which uses $\varepsilon(\omega)$ for an infinite crystal and fails to take into account modified physical properties at slab surfaces.

Microscopic theories (see [6] and references therein) have clearly demonstrated that SM persist at $k = 0$ if the modification of forces acting on surface ions is taken into account. It follows from microscopic theories that two types of SM should be distinguished [7]: SM of *the first type*, whose amplitudes decrease slowly with the distance from the surface; and SM of *the second type*, whose amplitudes decrease over distances of the order of the lattice constant a. Obviously, only SM of *the first type* can be described by a phenomenological macroscopic theory. These two types of SM are coupled; that coupling, however, can be neglected in the long-wavelength limit $ka \ll 1$ provided that their dispersion branches do not intersect each other [7]; numerical calculations for very thin films [6, 8] suggest that this is indeed the case. Another interesting effect which does not come out from a macroscopic theory is the interaction of SM and BM. That is, by means of a numerical analysis of the microscopic theory [6] the effect of anticrossing between the dispersion curves of SM and BM of the same symmetry can be seen; as the frequencies of the two modes of the same symmetry approach one another, they repel each other and their eigenvectors exchange character. It has been shown that the changes of frequency and the finite lifetime of SM of *the first type* due to the interaction with BM are effects of the order of ka [7]. A detailed review of macroscopic as well as microscopic theories can be found in [9].

Let us now discuss how the effect of the spatial dispersion, which in microscopic theories is taken into account in fact automatically, is usually included in the permittivity formalism. In this case, ε depends on the three-dimensional wavevector $\boldsymbol{q}$ due to the $\boldsymbol{q}$-dependence of ω_{t} in (1). The two-dimensional wavevector $\boldsymbol{k}$ involved is related to $\boldsymbol{q}$ through $\boldsymbol{q} = \boldsymbol{k} + q_z \boldsymbol{i_z}$, where $\boldsymbol{i_z}$ is a unit vector parallel to the z-axis. If the spatial dispersion is sufficiently small, i.e. $qa \ll 1$, and if we consider the dispersion of ω_{t} in the cubic crystal to be isotropic for simplicity, we take into account the spatial dispersion simply by replacing ω_{t}^2 in (1) by $\omega_{\mathrm{t}}^2(\boldsymbol{q}) = \omega_{\mathrm{t}}^2 + Dq^2$. In an infinite crystal, $\varepsilon(\omega, q)$ relates the field amplitudes of the plane waves to the wavevector $\boldsymbol{q}$, i.e., $\boldsymbol{D}(\omega, \boldsymbol{q}) = \varepsilon(\omega, q)\boldsymbol{E}(\omega, \boldsymbol{q})$, where

$$\varepsilon(\omega, q) = \varepsilon_\infty \frac{\omega_{\mathrm{l}}^2 + Dq^2 - \mathrm{i}\omega\gamma - \omega^2}{\omega_{\mathrm{t}}^2 + Dq^2 - \mathrm{i}\omega\gamma - \omega^2}. \tag{2}$$

This equation expresses a non-local relation between $\boldsymbol{D}$ and $\boldsymbol{E}$ which explains why, in a spatially dispersive crystal, normal modes can no longer be found from Maxwell's equations and the continuity of fields at the surfaces themselves; ABC containing information about the properties of the surface are needed. Various ABC have been introduced *ad hoc* (see [10] for example): either some components of $\boldsymbol{P}$ or the derivatives of P_i or, more generally, a linear combination of them vanish at the surfaces of the slab. However, it has been shown that, in the macroscopic theory using the permittivity formalism, new boundary conditions follow directly from the non-local form of Maxwell's equations and it is not necessary to construct a microscopic model of the crystal surface in order to complete the theory [11, 12] of the SM of *the first type*. In this theory the influence of the surface is only related to the loss of translational invariance in the z-direction and a non-local permittivity is obtained by partial Fourier transformation of $\varepsilon(\omega, q)$; other effects of the surface are not taken into account.

Instead, we shall follow a procedure commonly used in ferroelectric thin films [1] which specifies the physical properties of the surface and leads to realistic ABC. This procedure consists in introducing the spatial dispersion directly in the equations of motion for P_i:

$$m\frac{\partial^2 P_i}{\partial t^2} + \gamma\frac{\partial P_i}{\partial t} + m\omega_{\mathrm{t}}^2 P_i - C\left\{\left(\frac{\partial^2 P_i}{\partial x^2}\right) + \left(\frac{\partial^2 P_i}{\partial z^2}\right)\right\} = E_i. \tag{3}$$

These equations follow from the well known kinetic equation

$$m\frac{\partial^2 \boldsymbol{P}}{\partial t^2} + \gamma\frac{\partial \boldsymbol{P}}{\partial t} + \frac{\delta F}{\delta \boldsymbol{P}} = \boldsymbol{0} \tag{4}$$

restricted to the harmonic part of the Landau free-energy density in the appropriate simplified form:

$$F = \tfrac{1}{2}\sum_i \{m\omega_{\mathrm{t}}^2 P_i^2 + C(\nabla P_i)^2\} - \boldsymbol{E}\cdot\boldsymbol{P}. \tag{5}$$

Obviously, for the second-order differential equations, boundary conditions on P_i at the surfaces are needed [13]. Generalizing the boundary conditions used in [14], we take them in the form

$$\left[\frac{\partial P_i}{\partial z} \pm \frac{P_i}{\delta_i}\right]_{z=\pm d/2} = 0. \tag{6}$$

These ABC result in fact from the variation equations $\delta F/\delta P_i = 0$ if the volume energy density (5) is completed by the surface energy density:

$$\frac{C}{2}\sum_i \frac{P_i^2(z=-d/2) + P_i^2(z=+d/2)}{\delta_i}$$

which expresses the fact that the polarization energy at the surfaces is different from that of the bulk. Note that (3) defines a system of coupled equations for P_x and P_z. This is because for $k \neq 0$ the polarization wave P_x produces also a component of the electric field E_z acting on P_z and similarly the polarization wave P_z produces an E_x-component (explicit formulae for E_i can be found in [3]). The coupling between P_z and P_x was ignored by Cottam *et al* [14] and therefore their results only apply to the case of $k = 0$ where P_z and P_x are decoupled.

In the following section we shall work out in detail the procedure that we have just briefly described.

2. Theory

We consider an infinite slab of thickness d consisting of the material studied, of cubic symmetry, in contact with two semi-infinite isotropic dielectric media with dielectric constants ε_1 and ε_2 independent of the frequency (indeed, one of them or both can be replaced by vacuum), as shown in figure 1. In the present section we intend to study the propagation of electromagnetic waves whose wavevector lies in the (x, y) plane, looking for solutions of Maxwell's equations in which the components (labelled by $i = x, y, z$) do not depend of y and are of the following form:

$$U_i(\boldsymbol{r}, t) = U_i(z)\exp[\mathrm{i}(kx - \omega t)] \qquad \text{with } \boldsymbol{U} = \boldsymbol{E}, \boldsymbol{D}, \boldsymbol{P} \text{ or } \boldsymbol{H}. \tag{7}$$

The magnetic permeability is assumed to be equal to unity in all three media. We are interested only in the electromagnetic modes localized in the slab, i.e. for which $U_i(z) \to 0$ when $z \to \pm\infty$. As pointed out already in the introduction, these modes can be divided in two groups: (1) bulk modes (BM) for which the fields sinusoidally oscillate inside the slab; and (2) surface modes (SM) for which they exponentially decay with increasing distance from the surface. Finally, as usual, we have to consider two distinct configurations: (i) the case where the electric field lies in a plane parallel to the slab along the y-axis, which imposes $E_x = E_z = 0$, $H_y = 0$ (s polarization, sometimes defined as TE modes); and (ii) the case where the electric field lies in the sagittal plane, which imposes $E_y = 0$, $H_x = H_z = 0$ (p polarization or TM modes).

In the case of s modes the Maxwell equations

$$\mathrm{curl}(\boldsymbol{E}) = -\frac{1}{c}\frac{\partial \boldsymbol{H}}{\partial t} \qquad \text{and} \qquad \mathrm{curl}(\boldsymbol{H}) = \frac{1}{c}\frac{\partial \boldsymbol{D}}{\partial t} \tag{8}$$

lead to the following relations:

$$E_y''(z) - k^2 E_y(z) + \frac{\omega^2}{c^2} D_y(z) = 0 \tag{9a}$$

$$E_y'(z) = -\mathrm{i}\frac{\omega}{c} H_x(z) \tag{9b}$$

$$H_z(z) = \frac{ck}{\omega} E_y(z) \tag{9c}$$

while in the case of p modes we get

$$kE_x'(z) - \mathrm{i}k^2 E_z(z) + \mathrm{i}\frac{\omega^2}{c^2} D_z(z) = 0 \tag{10a}$$

$$\mathrm{i}kD_x(z) + D_z'(z) = 0 \tag{10b}$$

$$kH_y(z) = -\frac{\omega}{c} D_z(z) \tag{10c}$$

with

$$\boldsymbol{D} = \boldsymbol{E} + 4\pi \boldsymbol{P}.$$

In equations (9) and (10) we use the notation

$$\Phi' = \frac{\partial \Phi}{\partial z} \qquad \Phi'' = \frac{\partial^2 \Phi}{\partial z^2}.$$

Indeed, outside the slab,

$$\boldsymbol{P} = \begin{cases} \dfrac{\varepsilon_2 - 1}{4\pi}\boldsymbol{E} & \text{for } z > d/2 \\ \dfrac{\varepsilon_1 - 1}{4\pi}\boldsymbol{E} & \text{for } z < -d/2. \end{cases} \tag{11}$$

In the slab, the total polarization, now labelled $\boldsymbol{P}$ is

$$\boldsymbol{P}_{\rm T} = \boldsymbol{P}_{\rm el} + \boldsymbol{P} \tag{12}$$

where $\boldsymbol{P}_{\rm el}$ stands for an electronic frequency-independent part:

$$\boldsymbol{P}_{\rm el} = \frac{\varepsilon_\infty - 1}{4\pi} E \tag{13}$$

and where we assume, as pointed out in the introduction, that the frequency-dependent part of $\boldsymbol{P}$ is solution of a Landau–Ginzburg equation:

$$m\frac{\partial^2 \boldsymbol{P}}{\partial t^2} + \frac{\delta F}{\delta \boldsymbol{P}} = \boldsymbol{0}. \tag{14}$$

In the above equation, where damping is neglected, m is an inertial positive parameter and F is the appropriate free-energy density. In view of the required linearization, we consider only the harmonic part of the free energy which we write as (per unit area)

$$\Psi = \Psi_V + \Psi_S \tag{15a}$$

with

$$\Psi_V = \int \mathrm{d}x \int_{-d/2}^{+d/2} F\,\mathrm{d}z \tag{15b}$$

where

$$F = \frac{A(T)}{2}\boldsymbol{P}^2 - \boldsymbol{E}\cdot\boldsymbol{P} + \frac{C}{2}\left[\left(\frac{\partial P_x}{\partial x}\right)^2 + \left(\frac{\partial P_z}{\partial z}\right)^2\right] + \frac{C'}{2}\left[\left(\frac{\partial P_x}{\partial z}\right)^2 + \left(\frac{\partial P_y}{\partial x}\right)^2 + \left(\frac{\partial P_y}{\partial z}\right)^2 + \left(\frac{\partial P_z}{\partial x}\right)^2\right] + C''\frac{\partial P_x}{\partial x}\frac{\partial P_z}{\partial z} + C'''\frac{\partial P_x}{\partial z}\frac{\partial P_z}{\partial x} \tag{15c}$$

and

$$\Psi_S = \frac{C}{2}\left[\frac{P_x^2(x,d/2) + P_y^2(x,d/2)}{\delta_{x+}} + \frac{P_x^2(x,-d/2) + P_y^2(x,-d/2)}{\delta_{x-}} + \frac{P_z^2(x,d/2)}{\delta_{z+}} + \frac{P_z^2(x,-d/2)}{\delta_{z-}}\right]. \tag{15d}$$

In the case of a ferroelectric material, the above expression holds for the paraelectric phase with $A = \alpha(T - T_c)$ with $\alpha > 0$. In order to study the ferroelectric phase, A would have to be renormalized; however, due to finite-size effects it would depend upon z, which severely complicates further calculations. In the following, we neglect the cross gradient terms C'' and C'''; in addition we assume that $C' = C > 0$. Finally, we assume that the surface extrapolation lengths do not depend on the side considered, i.e. $\delta_{x+} = \delta_{x-} = \delta_x$; $\delta_{z+} = \delta_{z-} = \delta_z$. Notice, however, that we introduce two independent lengths, the in-plane one ($\delta_x = \delta_y$ in agreement with the symmetry) and the out-of-plane one δ_z.

In addition to equation (14), one has to take into account the boundary conditions at $z = \pm d/2$ arising from the continuity of the appropriate components of the fields and from the finite-size effects in the energy minimization. These last conditions can be written as

$$\left[\frac{\partial P_i}{\partial z} \pm \frac{P_i}{\delta_i}\right]_{z=\pm d/2} = 0 \qquad (i = x, y, z). \tag{16}$$

Throughout the rest of this section we shall discuss the p and the s solutions neglecting the retardation effects ($\omega/c = 0$: electrostatic approximation). Strictly speaking, for very small $|k|$-values such an approximation fails, since it assumes that $|k| \gg \omega/c$. However, the electrostatic approximation often provides for a large allowed range of physically small $|k|$-values (i.e. simultaneously subjected to $|kd| \ll 1$, to $|k\delta_i| \ll 1$ and to $Ck^2 \ll 1$) as the reported data [15] do not exceed a few tens of nm and a few tens of nm^2 for $|\delta_i|$ and for C, respectively; then, with a typical order of magnitude of a few 10^{13} rad s^{-1} for ω, the electrostatic approximation is satisfied for $|k| \gg 10^{-4}$ nm^{-1} while $|k|$ can be considered as small when it is significantly smaller than 10^{-2} nm^{-1}. Notice that the following considerations significantly generalize the content of our preliminary paper [16] concerning only $k = 0$ modes in the special case where $\delta_x^{-1} = 0$ and where, consequently, there are only p modes polarized along $\boldsymbol{z}$.

Using (7) and (15), equation (14) becomes

$$(-m\omega^2 + A + Ck^2)P_i(z) - CP_i'' = E_i(z). \tag{17}$$

The solutions of the form $E_i(z) = E_i \exp[\beta z]$, $P_i(z) = P_i \exp[\beta z]$ are then subject to

$$E_i = [W(k, \omega) - C\beta^2]P_i$$

with

$$W(k, \omega) = A(T) - m\omega^2 + Ck^2 = m(\omega_t^2 - \omega^2) + Ck^2 \tag{18}$$

where we have introduced the bulk transverse frequency ω_t.

The polarization modes propagating in the slab are linear combinations of these exponential solutions subject to the surface boundary conditions.

2.1. s modes

It follows from (9a), (9b) and (18) (with $i = y$) that

$$\begin{aligned} &[\beta^2 - k^2][W(k, \omega) - C\beta^2]P_y = 0 \\ &\beta E_y = 0. \end{aligned} \tag{19}$$

The solutions with non-zero polarization have to satisfy

$$\beta = \pm\beta_n \qquad (n = 1 \text{ or } 2) \qquad \text{with } \beta_1 = |k| \text{ and } \beta_2 = [W(k, \omega)/C]^{1/2}$$

with, necessarily, $\boldsymbol{E} = \boldsymbol{0}$. One easily shows that β_1 does not contribute to non-zero solutions. The allowed values for β_2 immediately result from equations (16). They are solutions of

$$\beta_2\delta_x = -\coth[\beta_2 d/2] \tag{20a}$$

or of

$$\beta_2\delta_x = -\tanh[\beta_2 d/2]. \tag{20b}$$

β_2 can be a *real* solution of

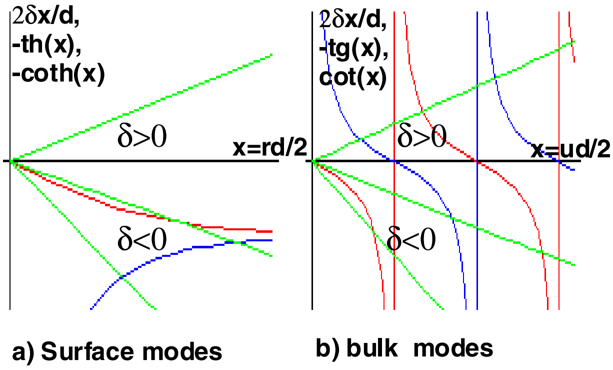

Figure 2. Graphical determination of β (see the text). We have omitted the indices e and o for even and odd (e relates to coth (or to cot), o relates to tanh (or to tan)). Depending upon the case studied, δ stands for δ_x or for δ_z.

$$r_e\delta_x = -\coth[r_e d/2] \qquad \text{with } \beta_2 = r_e \tag{21a}$$

or of

$$r_o\delta_x = -\tanh[r_o d/2] \qquad \text{with } \beta_2 = r_o. \tag{21b}$$

Alternatively, β_2 can be a *purely imaginary* solution of

$$u_e\delta_x = \cot[u_e d/2] \qquad \text{with } \beta_2 = iu_e \tag{22a}$$

or of

$$u_o\delta_x = -\tan[u_o d/2] \qquad \text{with } \beta_2 = iu_o. \tag{22b}$$

These solutions are graphically depicted in figure 2: it appears that real solutions only exist for $\delta_x < 0$ (except for $\beta_2 = 0$, which, as is easily seen, does not contribute to non-zero solutions). The indices e and o respectively label even and odd modes with respect to the change $z \to -z$. For the first ones, the polarization is proportional to $\cosh[r_e z]$ (real solutions $\to$ surface modes) or to $\cos[u_e z]$ (imaginary solutions $\to$ bulk modes). For the second ones, the polarization is proportional to $\sinh[r_o z]$ (real solutions $\to$ surface modes) or to $\sin[u_o z]$ (imaginary solutions $\to$ bulk modes). In both cases, the variation versus z of the polarization is independent of k.

It turns out from (18) that the frequencies of the surface modes can be written as

$$m\omega^2 = m\omega_t^2 - Cr^2 + Ck^2 \tag{23a}$$

and of the bulk modes as

$$m\omega^2 = m\omega_t^2 + Cu^2 + Ck^2. \tag{23b}$$

One also notices that the electric field cancels everywhere and that for $C = 0$ there are no non-zero solutions.

2.1.1. Even modes.

(i) $\delta_x < 0$. There is always only one even surface mode related to the unique real solution r_e of equation (21a) appearing in figure 2. The imaginary solutions connected to $u_{e,p}$, where the index p is any positive integer, define an infinite set of even bulk modes.

Indeed, the concept of surface mode is specially meaningful when the required scale for a significant decrease of the polarization is small compared to d. This condition is satisfied for $|\delta_x| \ll d$, which leads to

$$
\begin{aligned}
r_{\mathrm{e}} &\cong \frac{1}{|\delta_x|}\left(1+2\exp\left[-\frac{d}{|\delta_x|}\right]\right) \approx \frac{1}{|\delta_x|} \\
m\omega_{\mathrm{e}}^2 &\cong m\omega_{\mathrm{t}}^2 - \frac{C}{\delta_x^2}\left(1+4\exp\left[-\frac{d}{|\delta_x|}\right]\right) + Ck^2 \approx m\omega_{\mathrm{t}}^2 - \frac{C}{\delta_x^2} + Ck^2.
\end{aligned} \tag{24}
$$

When $|\delta_x| \gg d$, the variation of the amplitude of the polarization in the slab versus z remains small. In this case one finds

$$
r_{\mathrm{e}} \cong \sqrt{\frac{2}{d|\delta_x|}} \qquad m\omega_{\mathrm{e}}^2 \cong m\omega_{\mathrm{t}}^2 - \frac{2C}{d|\delta_x|} + Ck^2. \tag{25}
$$

For the bulk modes, $u_{\mathrm{e,p}}$ increases with p. For large p, one finds

$$
u_{\mathrm{e,p}} \cong p\frac{2\pi}{d} \qquad m\omega_{\mathrm{e,p}}^2 \cong m\omega_{\mathrm{t}}^2 + p^2\frac{4\pi^2 C}{d^2} + Ck^2. \tag{26}
$$

(ii) $\delta_x > 0$. There are no even surface modes. There is still an infinite set of bulk modes labelled by a positive integer p. For large values of p, the expressions (26) remain valid.

2.1.2. Odd modes. (i) $\delta_x < 0$. There is one surface mode only for $|\delta_x| < d/2$. When $|\delta_x|$ increases from below to above $d/2$, the surface mode transforms into a bulk mode. In any case there is an infinite set of odd bulk modes.

For $|\delta_x| \ll d$, one finds

$$
\begin{aligned}
r_{\mathrm{o}} &\cong \frac{1}{|\delta_x|}\left(1-2\exp\left[-\frac{d}{|\delta_x|}\right]\right) \approx \frac{1}{|\delta_x|} \\
m\omega_{\mathrm{o}}^2 &\cong m\omega_{\mathrm{t}}^2 - \frac{C}{\delta_x^2}\left(1-4\exp\left[-\frac{d}{|\delta_x|}\right]\right) + Ck^2 \approx m\omega_{\mathrm{t}}^2 - \frac{C}{\delta_x^2} + Ck^2.
\end{aligned} \tag{27}
$$

For large values of $d/|\delta_x|$ the frequency of the odd surface mode is nearly equal to the frequency of the even surface mode. In the general case its frequency, when it exists ($|\delta_x| < d/2$), is larger.

For the bulk modes, $u_{\mathrm{o,p}}$ increases with p. For large p, one finds

$$
\begin{aligned}
u_{\mathrm{o,p}} &\cong (2p \pm 1)\frac{\pi}{d} \qquad +\!: |\delta_x| < d/2 \qquad -\!: |\delta_x| > d/2 \\
m\omega_{\mathrm{o,p}}^2 &\cong m\omega_{\mathrm{t}}^2 + (2p \pm 1)^2\frac{\pi^2 C}{d^2} + Ck^2.
\end{aligned} \tag{28}
$$

(ii) $\delta_x > 0$. There are never odd surface modes. There is still an infinite set of bulk modes labelled by a positive integer p. For large values of p, the expressions (28) with the negative sign remain valid.

The above-discussed behaviour of the whole set of polarization modes at $k = 0$ is illustrated in figure 3, which shows the variations of $m(\omega^2 - \omega_{\mathrm{t}}^2)$ versus d calculated for $\delta_x = -3$ nm and $C = 500$ nm^2. The chosen value for $|\delta_x|$ agrees with published typical orders of magnitude [15]. In contrast, we adopted for C a value significantly larger than the generally admitted one in order to illustrate specific behaviours of the surface modes which are commented on in the following (see the subsection 2.2.2*a*).

2.2. p modes

From equations (10*a*), (10*b*), (10) and (18) one derives the relations

$$
\begin{aligned}
&\beta(W - C\beta^2)P_x - \mathrm{i}k(W - C\beta^2)P_z = 0 \\
&\mathrm{i}k\left(W + \frac{4\pi}{\varepsilon_\infty} - C\beta^2\right)P_x + \beta\left(W + \frac{4\pi}{\varepsilon_\infty} - C\beta^2\right)P_z = 0.
\end{aligned} \tag{29}
$$

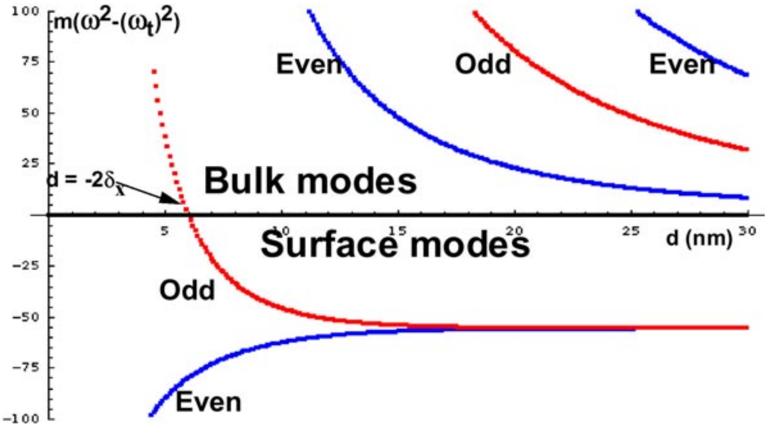

Figure 3. Variations of $m(\omega^2 - \omega_t^2)$ versus the film width d at $\boldsymbol{k} = \boldsymbol{0}$ for the modes showing a polarization parallel to the film. These variations are calculated for $C = 500$ nm^2, $\delta_x = -3$ nm. In the case of P_z-modes the curves represent the variations of $m(\omega^2 - \omega_l^2)$, assuming the same values of C and of δ_z.

This system admits non-zero solutions only if

$$[\beta^2 - k^2][W - C\beta^2]\left[W + \frac{4\pi}{\varepsilon_\infty} - C\beta^2\right] = 0. \tag{30}$$

It follows from equation (30) that β has to satisfy $\beta = \pm\beta_n$, $(n = 1, 2, 3)$, with

$$\beta_1 = |k| \qquad \beta_2 = \left[\frac{W}{C}\right]^{1/2} \qquad \beta_3 = \left[\frac{W + 4\pi/\varepsilon_\infty}{C}\right]^{1/2}. \tag{31}$$

We seek field components that are linear combinations of $\exp[\pm\beta_n z]$. More explicitly, it is convenient to write

$$P_x(z) = \frac{\mathrm{i}k}{\beta_1}(a_{1\mathrm{e}}\cosh[\beta_1 z] + a_{1\mathrm{o}}\sinh[\beta_1 z]) + (a_{2\mathrm{e}}\cosh[\beta_2 z] + a_{2\mathrm{o}}\sinh[\beta_2 z]) + \frac{\mathrm{i}k}{\beta_3}(a_{3\mathrm{e}}\cosh[\beta_3 z] + a_{3\mathrm{o}}\sinh[\beta_3 z]). \tag{32}$$

$P_z(z)$ is derived from equation (29):

$$P_z(z) = (a_{1\mathrm{e}}\sinh[\beta_1 z] + a_{1\mathrm{o}}\cosh[\beta_1 z]) - \mathrm{i}\frac{k}{\beta_2}(a_{2\mathrm{e}}\sinh[\beta_2 z] + a_{2\mathrm{o}}\cosh[\beta_2 z]) + (a_{3\mathrm{e}}\sinh[\beta_3 z] + a_{3\mathrm{o}}\cosh[\beta_3 z]). \tag{33}$$

The indices e and o stand for even and odd, respectively, referring to P_x: notice that they correspond to odd and even components, respectively, when referring to P_z. The components of the electric field are immediately found from equations (10*a*) and (10*b*). Outside the slab the field components have to be proportional to $\exp[-|kz|]$ in order to vanish at infinity: it then follows from Maxwell's equations and from equation (11) that the external fields depend only upon one coefficient on each side. Writing the continuity equations for E_x and D_z and the boundary conditions of equation (16) for P_x and P_z at $z = \pm d/2$, one finally obtains a set of eight equations which reduce to a homogeneous set of six linear equations for the six coefficients ($a_{1\mathrm{e}}$ to $a_{3\mathrm{o}}$) introduced in equation (32). An implicit expression for the frequencies of the modes is then obtained through the vanishing of the determinant of a 6×6 matrix **M** (see table 1). At this stage, in the general case, numerical calculations are necessary. However,

Table 1. The expression for the matrix $\mathbf{M}$ of the coefficients of the homogeneous system of equations allowing the calculation of the frequencies. $\mathbf{M}_{\mathrm{ez,ox}}$ is immediately derived from $\mathbf{M}_{\mathrm{ex,oz}}$ by changing cosh into sinh and vice versa. $\mathbf{M}_{\mathrm{as}}^{(2)}$ is derived from $\mathbf{M}_{\mathrm{as}}^{(1)}$ by changing sinh into cosh.

$$\mathbf{M} = \begin{bmatrix} \mathbf{M}_{\mathrm{ex,oz}} & \mathbf{M}_{\mathrm{as}}^{(1)} \\ \mathbf{M}_{\mathrm{as}}^{(2)} & \mathbf{M}_{\mathrm{ez,ox}} \end{bmatrix} \quad \text{with:}$$

$$\mathbf{M}_{\mathrm{ex,oz}} = \begin{bmatrix} \begin{array}{l}(\varepsilon_1+\varepsilon_2)C(k^2-\beta_2^2)\cosh[kd/2] \\ \quad + 2\varepsilon_\infty C(k^2-\beta_3^2)\sinh[|k|d/2]\end{array} & \mathrm{i}\,8\pi\frac{k}{\beta_2}\sinh[\beta_2 d/2] & (\varepsilon_1+\varepsilon_2)\frac{4\pi}{\varepsilon_\infty}\frac{|k|}{\beta_3}\cosh[\beta_3 d/2] \\ |k|\cosh[kd/2] + \frac{\sinh[|k|d/2]}{\delta_z} & -\mathrm{i}k\left(\cosh[\beta_2 d/2] + \frac{\sinh[\beta_2 d/2]}{\beta_2\delta_z}\right) & \beta_3\cosh[\beta_3 d/2] + \frac{\sinh[\beta_3 d/2]}{\delta_z} \\ \mathrm{i}\left(k\sinh[|k|d/2] + \frac{k}{|k|}\frac{\cosh[kd/2]}{\delta_x}\right) & \beta_2\sinh[\beta_2 d/2] + \frac{\cosh[\beta_2 d/2]}{\delta_x} & \mathrm{i}k\left(\sinh[\beta_3 d/2] + \frac{\cosh[\beta_3 d/2]}{\beta_3\delta_x}\right) \end{bmatrix}$$

$$\mathbf{M}_{\mathrm{as}}^{(1)} = \begin{bmatrix} (\varepsilon_1-\varepsilon_2)C(k^2-\beta_2^2)\sinh[|k|d/2] & 0 & (\varepsilon_1-\varepsilon_2)\frac{4\pi}{\varepsilon_\infty}\frac{|k|}{\beta_3}\sinh[\beta_3 d/2] \\ 0 & 0 & 0 \\ 0 & 0 & 0 \end{bmatrix}$$

there are considerable simplifications at zero wavevector. For $k \neq 0$, the case of a symmetrical environment of the slab ($\varepsilon_1 = \varepsilon_2$) can be rather easily studied: the 6×6 matrix $\mathbf{M}$ splits into two 3×3 matrices $\mathbf{M}_{\mathrm{ex,oz}}$ and $\mathbf{M}_{\mathrm{ez,ox}}$, reflecting the occurrence of two systems of independent equations related to even and odd modes related to the P_x-components, respectively involving $(a_{1\mathrm{e}}, a_{2\mathrm{e}}, a_{3\mathrm{e}})$ and $(a_{1\mathrm{o}}, a_{2\mathrm{o}}, a_{3\mathrm{o}})$. Finally, for small $|k|$, linear dependences of the frequencies on $|k|$ can be obtained.

2.2.1. The special case $k = 0$. In this case, the matrix $\mathbf{M}$ has a very simple form which gives rise to a complete decoupling between the P_x- and the P_z-components. More specifically, even for $\varepsilon_1 \neq \varepsilon_2$, $\mathbf{M}$ splits into two matrices $\mathbf{M}_{\mathrm{ex,oz}}$ and $\mathbf{M}_{\mathrm{ez,ox}}$. $\mathbf{M}_{\mathrm{ex,oz}}$ is related to two distinct sets of modes: even-P_x modes with $P_z = 0$ and odd-P_z modes with $P_x = 0$. Indeed $\mathbf{M}_{\mathrm{ez,ox}}$ describes odd-P_x and even-P_z modes. The determinant of $\mathbf{M}$, which, in fact, is the product of the determinants of the two sub-matrices can be written as

$$\Delta(0) = \beta_2^2\beta_3^2\left(\beta_2\delta_x + \coth\left[\beta_2\frac{d}{2}\right]\right)\left(\beta_2\delta_x + \tanh\left[\beta_2\frac{d}{2}\right]\right) \times \left(\beta_3\delta_z + \coth\left[\beta_3\frac{d}{2}\right]\right)\left(\beta_3\delta_z + \tanh\left[\beta_3\frac{d}{2}\right]\right). \tag{34}$$

The frequencies are obtained by equating to zero any of the factors appearing in (34): however, it is easy to show that $\beta_2 = 0$ and $\beta_3 = 0$ do not induce non-zero solutions.

Among the remaining factors the first two define the P_x-modes (even and odd modes, related to the factors containing coth and tanh, respectively). The discussion is identical to the preceding one concerning the s modes at $k = 0$. Indeed, at zero wavevector one finds a degeneracy between the P_x- and P_y-modes.

The two last factors define the P_z-modes (here again, even and odd modes are related to the factors containing coth and tanh, respectively). The discussion is completely analogous to the previous one. We just have to make the replacements

$$\delta_x \to \delta_z \qquad \text{and} \qquad m\omega_{\mathrm{t}}^2 \to m\omega_{\mathrm{l}}^2 = m\omega_{\mathrm{t}}^2 + \frac{4\pi}{\varepsilon_\infty}.$$

However, one has to notice that the electric field vanishes in the P_x-modes, while $E_z = -4\pi P_z/\varepsilon_\infty$ in the P_z-modes. These conclusions can be more easily derived from a direct examination of equation (29).

To summarize this subsection, we now have two sets of modes: P_x and P_z. Each set always presents bulk modes and, if the extrapolation length concerned is negative, one or two surface modes. The intricacy of the frequencies, which are insensitive to the values of ε_1 and of ε_2, depends upon the characteristic parameters of the slab. The lowest frequency is always associated with an even mode. In the case where both δ_x and δ_z are negative and show an absolute value very much smaller than d, the fundamental mode at $k = 0$ is of even-P_x type if $C/\delta_x^2 > C/\delta_z^2 - 4\pi/\varepsilon_\infty$ and of even-P_z type if $C/\delta_x^2 < C/\delta_z^2 - 4\pi/\varepsilon_\infty$.

2.2.2. Non-zero wavevectors. For $k \neq 0$, there is a coupling between the P_x- and the P_z-components. On the other hand, the frequencies and the variations versus z of the polarization components now become dependent on ε_1 and on ε_2.

(a) Symmetrical surroundings: $\varepsilon_1 = \varepsilon_2 = \varepsilon$. In this case, as pointed out above, for any given mode, the two components of the polarization show definite parities opposite to those of each other. In principle, their dependences on z may show a complicated profile, due to the occurrence of three hyperbolic and/or trigonometric functions in their expressions; notice that, strictly speaking, the distinction between surface modes and bulk modes may be incorrect. However, it is interesting to follow the evolution of the behaviour of the modes defined in the preceding subsection, when increasing $|k|$ from 0, at least up to moderate values.

Figure 4 shows the variations of $m(\omega^2 - \omega_t^2)$ versus $|k|$ for the four surface modes, calculated using $\delta_x = \delta_z = -3$ nm, $C = 500$ nm^2, $d = 25$ nm, $\varepsilon = 1$, $\varepsilon_\infty = 1$. For small $|k|$-values ($|kd|$ smaller than about 0.2), one observes that these variations are linear for the even-P_x and the even-P_z modes, while they depend quadratically on k for the odd modes, as justified below. For large $|k|$-values, the frequencies become close to each other, and their variations seem to be monitored by a term which is written as Ck^2 (as for the TE modes studied above, where the shift of $m\omega^2$ is exactly equal to Ck^2). Notice that, to simplify the study, we chose a value of C large enough to prevent the occurrence of guided bulk modes in the interval separating the surface P_x- and P_z-modes and, consequently, to prevent surface–bulk mixing: this is realized for $(C/d^2)\pi\varepsilon_\infty > 1$. Of course, this set of parameters does not allow one to achieve a satisfactory bulk permittivity ε_B since, as easily shown, $4\pi\delta^2/\{C(\varepsilon_B - \varepsilon_\infty)\}$ has to be positive in order to get $\omega^2 > 0$. Using a more realistic value for C would not drastically change the dispersion curves of the surface modes, at least at small $|k|$.

It follows from figure 4 that the lowest frequency occurs at zero wavevector both for the P_x- and the P_y-even branch. The frequencies of the P_z-modes are higher because of the depolarizing field produced by surface charges. Therefore, for a ferroelectric film in which $\delta_x = \delta_z$, the spontaneous polarization should develop in the x, y plane. This is valid as long as $C/\delta_x^2 > C/\delta_z^2 - 4\pi/\varepsilon_\infty$. In the case $C/\delta_x^2 < C/\delta_z^2 - 4\pi/\varepsilon_\infty$, the lowest branch is the P_z-even one and its minimum occurs at $k \neq 0$: a modulated spontaneous polarization should develop along the z-axis. This would be true only in the idealized situation when the surface charges would be not compensated due to conductivity of the film or external charges. On the other hand, in a short-circuited film the P_z-even mode at $k \neq 0$ would show a lower frequency due to the reduction of the depolarizing field which can be calculated using for instance the method of images [17].

The non-zero component (x or z) of $\boldsymbol{P}$ at $k = 0$ remains the principal one for moderate values of $|k|$. This is illustrated in figure 5 where we have shown the dependences on z of P_x and of P_z associated with the even fundamental surface mode for different values of $|k|$ (with the same parameters as in figure 4): the profile of P_x remains practically unchanged; $|P_z|/|P_x|$ keeps a small value which increases versus $|k|$. We observe a similar behaviour for the bulk modes, as shown in figure 6.

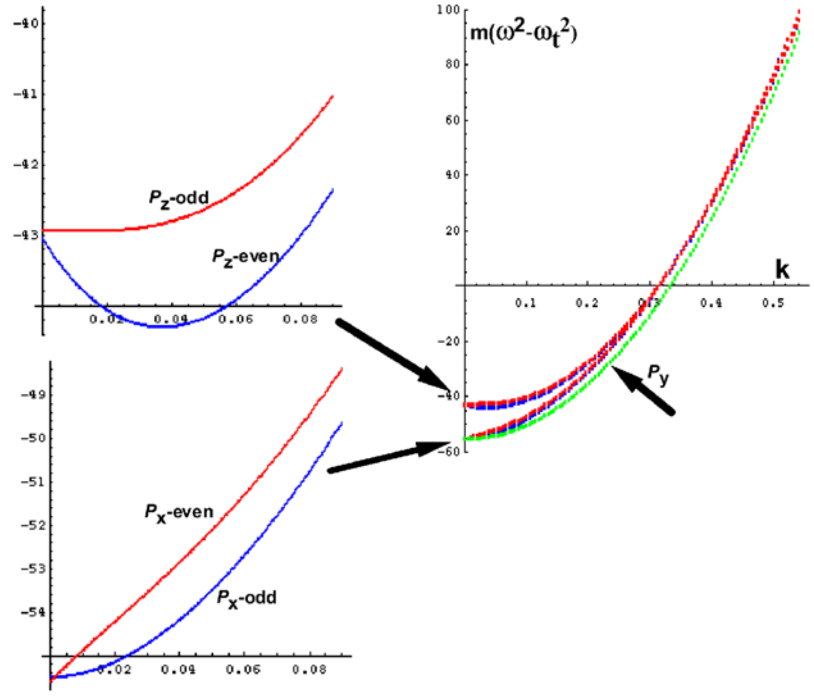

Figure 4. Dispersion curves of the surface polarization modes calculated using the following values: $C = 500$ nm^2; $\delta_x = \delta_z = -3$ nm; $\varepsilon_1 = \varepsilon_2 = 1$; $\varepsilon_\infty = 1$; $d = 25$ nm. The small splitting between the even and the odd P_y-modes is not shown.

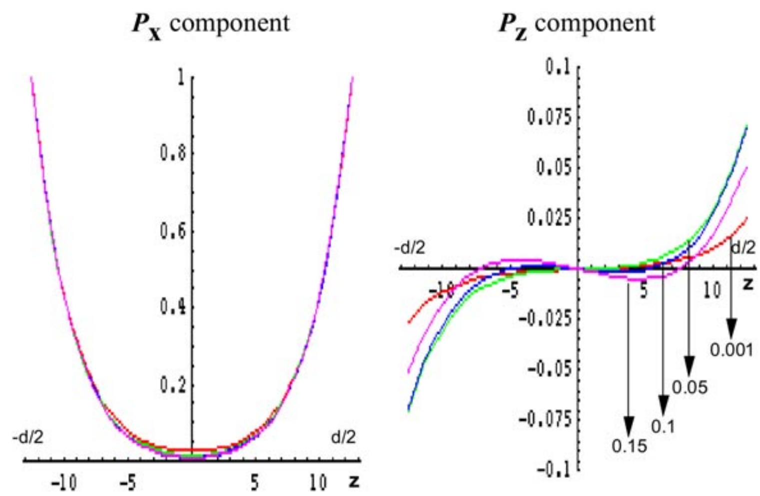

Figure 5. Mixing with increasing k between the P_x- and the P_z-components of a surface mode. The curves represent the variations versus z of the P_x-component and of the P_z-component of the lowest surface mode (P_x at $k = 0$) for increasing wavevectors (0.001, 0.05, 0.1, 0.15 nm^{-1}) calculated with $C = 500$ nm^2; $\delta_x = \delta_z = -3$ nm; $d = 25$ nm; $\varepsilon_1 = \varepsilon_2 = \varepsilon_\infty = 1$. The P_x-profile is practically independent of k; the P_z-component, which vanishes at $k = 0$, increases versus k.

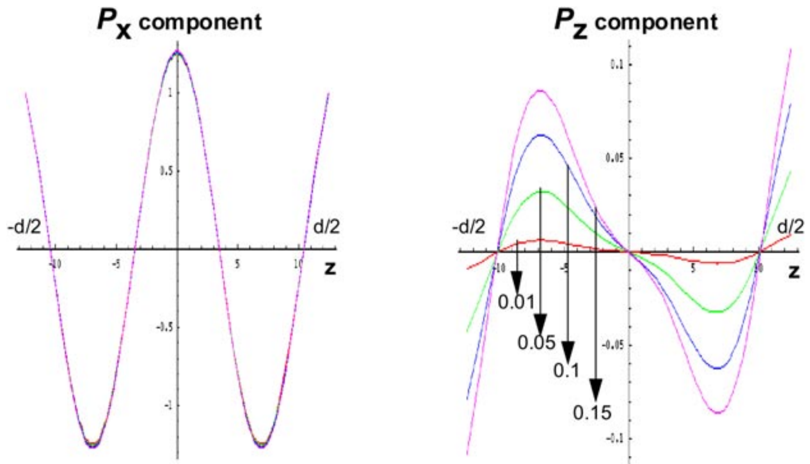

Figure 6. Mixing with increasing k between the P_x-component and the P_z-component of a bulk mode. The curves represent the variations versus z of the P_x-component and of the P_z-component of one of the bulk modes (P_x at $k = 0$) for increasing wavevectors (0.001, 0.05, 0.1, 0.15 nm^{-1}) calculated for $C = 500$ nm^2; $\delta_x = \delta_z = -3$ nm; $d = 25$ nm; $\varepsilon_1 = \varepsilon_2 = \varepsilon_\infty = 1$. The P_x-profile is practically independent of k, while the P_z-component, which vanishes at $k = 0$, increases versus k.

(b) Asymmetrical surroundings: $\varepsilon_2 \neq \varepsilon_1$. Except when $k = 0$, the polarization components do not show a definite parity any longer. The calculations have to be performed using the complete 6×6 matrix **M**. Figure 7 shows, in the case of the $k = 0$ even surface mode, the compared variations of $m(\omega^2 - \omega_t^2)$ versus $|k|$ for $\varepsilon_2 = 1$ and for $\varepsilon_2 = 12$ (keeping $\varepsilon_1 = 1$ in both cases).

When $\varepsilon_2 \neq \varepsilon_1$, very small values of $|k|$ are sufficient to break the symmetry properties, as shown in figure 8 which presents the profiles of the principal components of the two lowest surface modes ($k = 0$ even-P_x and odd-P_x modes) calculated with $\varepsilon_1 = 1$, $\varepsilon_2 = 12$. The frequencies of these two modes remain extremely close to each other, but their profiles change drastically when $|k|$ increases, even for small values of $|k|$. For $|k| = 10^{-3}$ nm^{-1}, the even and odd characters are still approximately preserved. This is no longer the case for $|k| = 10^{-2}$ nm^{-1}: the polarization is practically confined to one side of the slab (different sides for the two modes).

(c) Small $|k|$-values. We have expanded the determinant of **M** to first order in $|k|$, which allowed us to calculate the term linear in $|k|$ in the expressions for $m\omega^2$ relating to the p modes. This term exactly vanishes for the odd modes (thus confirming the behaviour shown in figure 4).

Let us discuss the results concerning the surface modes when both surface P_x-modes and surface P_z-modes exist, i.e. when both δ_x and δ_z are negative. In the case where $|\delta_x| \ll d$, $|\delta_z| \ll d$, one finds:

$$
\begin{aligned}
&\text{even } P_x: && m\omega^2 = m\omega_t^2 - \frac{C}{\delta_x^2} + \frac{16\pi}{\varepsilon_1 + \varepsilon_2}|\delta_x||k| + \mathrm{o}(k^2)\\
&\text{odd } P_x: && m\omega^2 = m\omega_t^2 - \frac{C}{\delta_x^2} + \mathrm{o}(k^2)\\
&\text{even } P_z: && m\omega^2 = m\omega_t^2 + \frac{4\pi}{\varepsilon_\infty} - \frac{C}{\delta_z^2} - \frac{16\pi}{\varepsilon_\infty^2}\frac{\varepsilon_1\varepsilon_2}{\varepsilon_1 + \varepsilon_2}|\delta_z||k| + \mathrm{o}(k^2)\\
&\text{odd } P_z: && m\omega^2 = m\omega_t^2 + \frac{4\pi}{\varepsilon_\infty} - \frac{C}{\delta_z^2} + \mathrm{o}(k^2).
\end{aligned}
\tag{35}
$$

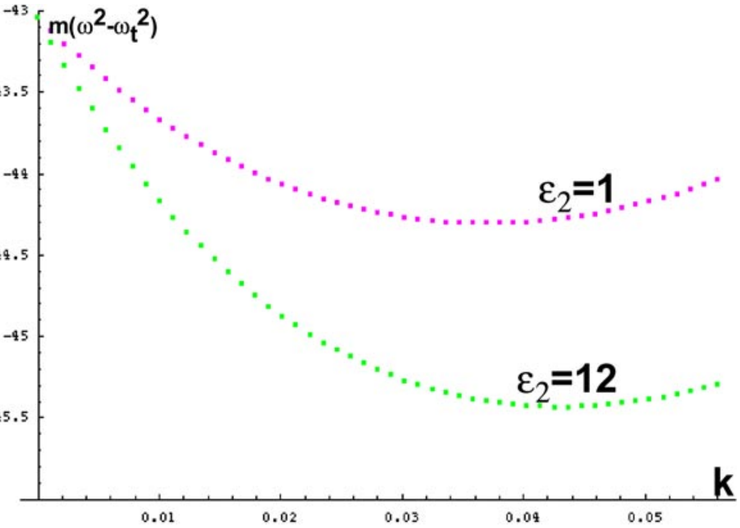

Figure 7. The influence of an unsymmetrical surroundings upon the dispersion curves. The variation of $m(\omega^2 - \omega_t^2)$ versus k for the even-P_z (at $k = 0$) mode is shown for $\varepsilon_1 = \varepsilon_2 = 1$ (symmetrical surroundings) and for $\varepsilon_1 = 1$, $\varepsilon_2 = 12$ (unsymmetrical surroundings). We use for the other parameters: $C = 500$ nm^2; $\delta_x = \delta_z = -3$ nm; $d = 25$ nm; $\varepsilon_\infty = 1$.

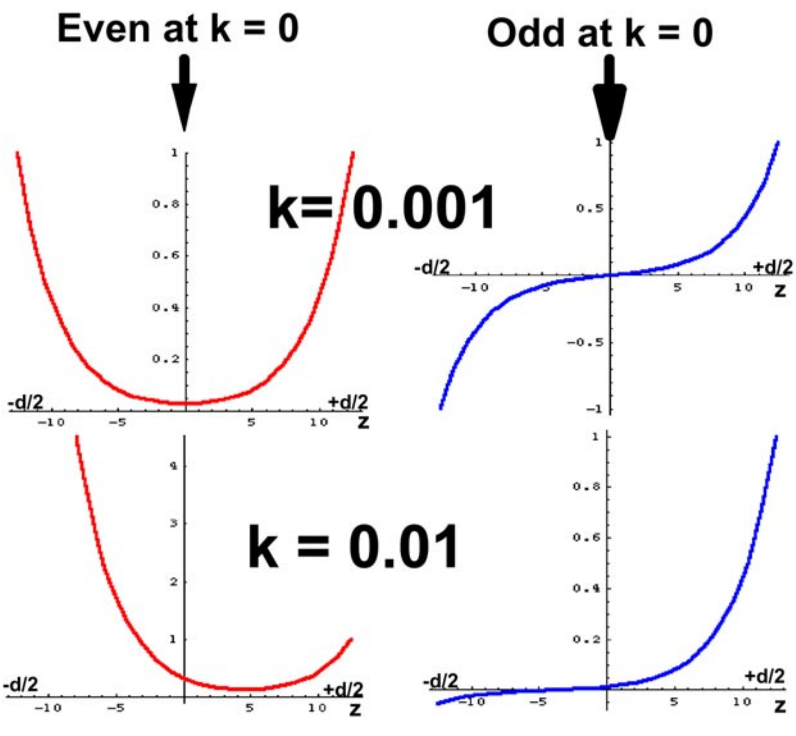

Figure 8. Symmetry breaking of the polarization profiles for unsymmetrical surroundings. The curves represent the variation versus z of the x-components of the two surface P_x-modes, calculated for: $\varepsilon_1 = 1$; $\varepsilon_2 = 12$ (other parameters: $C = 500$ nm^2; $\delta_x = \delta_z = -3$ nm; $d = 25$ nm; $\varepsilon_\infty = 1$).

In these expressions, we have neglected exponential terms similar to those that appear in (24).

In the opposite case where $|\delta_x| \gg d$, $|\delta_z| \gg d$, where only even surface modes are present, one finds

$$\begin{aligned} &\text{even } P_x: \qquad m\omega^2 = m\omega_{\mathrm{t}}^2 - 2\frac{C}{|\delta_x|d} + \frac{4\pi}{\varepsilon_1+\varepsilon_2}d|k| + \mathrm{o}(k^2) \\ &\text{even } P_z: \qquad m\omega^2 = m\omega_{\mathrm{t}}^2 + \frac{4\pi}{\varepsilon_\infty} - 2\frac{C}{|\delta_z|d} - \frac{4\pi}{\varepsilon_\infty^2}\frac{\varepsilon_1\varepsilon_2}{\varepsilon_1+\varepsilon_2}d|k| + \mathrm{o}(k^2). \end{aligned} \tag{36}$$

2.3. The surface waves of a semi-infinite medium

In order to allow for a more complete comparative discussion, we also sought for surface modes in a semi-infinite medium assumed to be identical to the slab described above and to occupy the $z < 0$ half-space (figure 1). The $z > 0$ half-space is supposed to be filled with an isotropic dielectric of dielectric constant ε. Now the energy minimization leads to only one surface boundary condition (at $z = 0$), namely

$$\left[\frac{\partial P_i}{\partial z} + \frac{P_i}{\delta_i}\right]_{z=0} = 0 \qquad (i = x, y, z; \delta_y = \delta_x). \tag{37}$$

In complete analogy with the case of a slab, we look for solutions of the form (7) where the dependences on z of the components of the fields are linear combinations of exponential functions. However, we have now to satisfy the vanishing of the fields at infinity not only in the dielectric ($z \to +\infty$) but also in the medium ($z \to -\infty$). Consequently, taking into account that the frequencies of the modes have to be real, the exponents of the exponential functions are required to be real and positive. Here again, one easily finds surface s modes as well as surface p modes.

s modes. They exist only for $\delta_x < 0$. They show a zero electric field and a polarization that decays as $\exp[r_{si}z]$ with a frequency $\omega_{si}(k)$ such that

$$r_{si} = \frac{1}{|\delta_x|} \qquad \text{and} \qquad m\omega_{si}^2 = m\omega_{\mathrm{t}}^2 - \frac{C}{\delta_x^2} + Ck^2. \tag{38}$$

This results for the frequency are the same as the values for the s modes in a slab found when $d \to \infty$ (see equations (24) or (27)).

p modes. In the case $k = 0$, one should distinguish between the P_x-mode and the P_z-mode as in a slab. The first one behaves in exactly the same way as the s modes just described (at $k = 0$). The P_z-mode is deduced from the P_x-mode by making the replacements

$$\delta_x \to \delta_z \qquad \text{and} \qquad m\omega_{\mathrm{t}}^2 \to m\omega_{\mathrm{l}}^2 = m\omega_{\mathrm{t}}^2 + \frac{4\pi}{\varepsilon_\infty}.$$

Both modes exist if δ_x and δ_z are negative.

At $k \neq 0$, there is a coupling between the P_x- and P_z-components. Each one is a linear combination of three exponentially decaying functions with exponents $\beta_n z$, where the β_n are respectively given by the three equations (31). Using an approach similar to the detailed one concerning the slab, we obtain the eigenfrequencies from the vanishing of a determinant of an appropriate 3×3 matrix $\mathbf{M}_\infty$ (given in table 2). For small k-values this determinant can be written as

$$\begin{aligned} \Delta_\infty = {} & [4\pi + (1+\varepsilon_\infty)W(0,\omega)]\left[\beta_2 + \frac{1}{\delta_x}\right]\left[\beta_3 + \frac{1}{\delta_z}\right] \\ & + 4\pi\left[\frac{1}{\varepsilon_\infty}\frac{1}{\beta_3\delta_z}\left(\beta_2 + \frac{1}{\delta_x}\right) - \frac{1}{\beta_2\delta_x}\left(\beta_3 + \frac{1}{\delta_z}\right)\right]|k|. \end{aligned} \tag{39}$$

Table 2. The matrix of the coefficients of the homogeneous system of linear equations involved in the case of a semi-infinite medium.

$$\mathbf{M}_\infty = \begin{bmatrix} \mathrm{i}\,4\pi\dfrac{k}{\beta_2} & -\dfrac{-4\pi}{\varepsilon_\infty}\dfrac{|k|}{\beta_3} & 4\pi-(1+\varepsilon_\infty)C(k^2-\beta_2^2) \\ \mathrm{i}k\left(1+\dfrac{1}{\beta_2\delta_z}\right) & \beta_3+\dfrac{1}{\delta_z} & |k|+\dfrac{1}{\delta_z} \\ -\left(\beta_2+\dfrac{1}{\delta_x}\right) & \mathrm{i}k\left(1+\dfrac{1}{\beta_3\delta_x}\right) & \mathrm{i}\left(k+\dfrac{k}{|k|}\dfrac{1}{\delta_x}\right) \end{bmatrix}$$

At $k = 0$ one recovers the frequencies of the P_x-mode and of the P_z-mode, respectively related to $\beta_2 = -1/\delta_x$ and $\beta_3 = -1/\delta_z$. Using equation (39), one easily finds the frequencies of the quasi-P_x-mode and of the quasi-P_z-mode for small k:

$$\begin{aligned} &P_x-\text{mode:}\quad m\omega^2 = m\omega_\mathrm{t}^2 - \frac{C}{\delta_x^2} + \left[\frac{8\pi}{(1+\varepsilon_\infty)}\right]\frac{|\delta_x|}{[1+4\pi\delta_x^2/C(1+\varepsilon_\infty)]}|k| \\ &P_z-\text{mode:}\quad m\omega^2 = m\omega_\mathrm{t}^2 + \frac{4\pi}{\varepsilon_\infty} - \frac{C}{\delta_z^2} - \left[\frac{8\pi}{\varepsilon_\infty(1+\varepsilon_\infty)}\right]\frac{|\delta_z|}{[1-4\pi\delta_z^2/C\varepsilon_\infty(1+\varepsilon_\infty)]}|k|. \end{aligned} \tag{40}$$

Notice that the term linear in $|k|$ differs from the expression derived from equation (35) obtained for a slab in which $|\delta_x| \ll d$, $|\delta_z| \ll d$.

Finally, at $k = 0$, the determinant Δ_∞ vanishes for $[4\pi + (1+\varepsilon_\infty)W] = 0$. However, this root does not correspond to a non-zero solution for the fields. In the next section we shall discuss the nature of the corresponding mode at small $|k|$.

3. Discussion and comparison with previous results

First, in the case where $C = 0$, our results expressed in equation (36), for a film, are in agreement with the theory of surface modes in ionic crystals, whose frequencies are given by [2]

$$\varepsilon(\omega) = -\frac{\varepsilon_1+\varepsilon_2}{2}\coth[kd]\left(1 \pm \left\{1 - 4\frac{\varepsilon_1\varepsilon_2}{(\varepsilon_1+\varepsilon_2)^2}\tanh^2[kd]\right\}^{1/2}\right) \tag{41}$$

where

$$\varepsilon(\omega) = \varepsilon_\infty + \frac{\omega_p^2}{\omega_\mathrm{t}^2-\omega^2} = \varepsilon_\infty\frac{\omega_\mathrm{l}^2-\omega^2}{\omega_\mathrm{t}^2-\omega^2}.$$

Noticing that

$$\omega_\mathrm{t}^2 = \frac{A(T)}{m} \qquad \omega_p^2 = \frac{4\pi}{m} \qquad \left(\text{and thus } \omega_\mathrm{l}^2 = \omega_\mathrm{t}^2 + \frac{4\pi}{m\varepsilon_\infty}\right) \tag{42}$$

equation (41) leads to equation (36) with $C = 0$ for small values of $|k|$.

Let us now compare our results with those obtained by Cottam *et al* [14] who also used the Landau–Ginzburg formalism but with the simplifying hypothesis of a scalar order parameter consisting of a non-specified component of the polarization; thus, they do not take account of the Maxwell's equations which, among other consequences, mix the components. For the s modes we get the behaviour calculated by Cottam *et al*, as expected, since for the s modes there is only one non-zero component of the polarization. For the p modes, the model of Cottam *et al* cannot predict the fourfold multiplicity of the surface modes, the splitting between the P_x- and the P_z-modes at zero wavevector and the dispersion of the frequencies versus $|k|$; however, for large k-values, in our model this dispersion is mainly governed by a quadratic term (that is, the variation of $m\omega^2$ follows the variation of Ck^2) identical in the two models. An important point to be noticed in our approach consists in the introduction of two independent extrapolation lengths, the in-plane one and the out-of-plane one, in agreement with the symmetry of the problem. Finally, our model could be developed beyond the electrostatic approximation while such a generalization has no meaning in the treatment of Cottam *et al*. However, calculations including retardation effects are rather tedious: anyway, it would be interesting to investigate whether the propagating modes disappear at small enough $|k|$-values, as observed in the absence of gradient terms in the free energy [4].

It is also of interest to compare our results with those obtained by Maradudin and Mills [12] using the dispersive permittivity formalism. First, obviously, for an infinite medium in the absence of any boundary surface, our equations of motion lead to a wavevector-dependent permittivity whose form is identical to the one proposed by those authors (the parameter C/m, related to the gradient term in our expression of the free energy, has to be identified with the parameter D appearing in equation (2) of section 1). To progress in the comparison we now restrict ourselves to the case of a semi-infinite medium described in section 2.3, since Maradudin and Mills did not study the case of a slab. In both models, the solutions can be expressed as linear combinations of three identical exponential functions. We showed that the existence of true surface modes necessitates introducing ABC taking into account negative density of surface energy. Maradudin and Mills were interested in the frequency region between ω_t and ω_l where the surface modes occur in the absence of spatial dispersion. In this case, it immediately follows from equation (30) that, at least for small k-values, two exponents are real and one is purely imaginary. The latter corresponds to the bulk polariton. The boundary conditions, however, admix a surface mode with the bulk polariton; consequently, the energy leaks of the surface into the bulk and it follows that the pseudo-surface mode is damped, even if the dielectric film is lossless. In our approach, we did not attempt to study these pseudo-surface modes and we focused on the true surface mode—that is to say, we explicitly sought for real exponential functions in order to get real frequencies and proper vanishing at infinity. Moreover, our model is rather different: we assume that the surface is a source of an additional localized surface energy term while they consider that it only restricts the spatial range of the interactions.

Finally, notice that we are able to get the usual frequency of the surface mode in a semi-infinite dielectric medium, which, in the absence of spatial dispersion is given by

$$\omega_\infty^2 = \omega_\mathrm{t}^2 + \frac{4\pi}{m(1+\varepsilon_\infty)} \tag{43}$$

using the notation of equations (42). This exactly corresponds to one of the roots for which the determinant of equation (39) vanishes at $k = 0$. For small C, it is easy to derive from (39) an approximate expression for the corresponding dispersion to first order in $|k|$. One finds

$$\omega^2 = \omega_\infty^2 + \left(\frac{1}{\delta_x} + \frac{1}{\delta_z}\right)\frac{C}{m}\left\{1 + \mathrm{i}\sqrt{\frac{1+\varepsilon_\infty}{4\pi}}\,\frac{\delta_z C^{1/2}}{\delta_x(\delta_x+\delta_z)}\right\}|k| \qquad (\text{assuming } C \ll \delta_x^2, \delta_z^2). \tag{44}$$

This root was not taken into account in section 2 since it does not provide for a solution vanishing at infinity. Expression (44) contains a small imaginary term which can be neglected and the linear shift

$$\Delta\omega = \left(\frac{1}{\delta_x} + \frac{1}{\delta_z}\right)\frac{C}{2m\omega_\infty}|k| \tag{45}$$

provides a good approximation only when $|k\delta_i| \ll 1$.

The main interest of our model concerns ferroelectric materials, because clearly in ferroelectric films the physical properties are strongly modified in the vicinity of the surfaces: the easiest phenomenological way to take these modifications into account consists in introducing surface energies, as done by many authors. In this context, we have proved that true surface polarization modes can be obtained only when the extrapolation lengths relating to these energies are negative, while such modes are absent for positive lengths. We have shown that in order to properly describe the polarization waves in thin films, it is necessary to introduce two independent extrapolation lengths for each boundary surface, thus generalizing previous studies based on a scalar order parameter.

Finally, in most of the experimental studies the static polarization in ferroelectrics is claimed to decrease in the vicinity of the surface, which argues for positive extrapolation lengths and, consequently, for the absence of true surface modes. But it seems that there exist a few exceptions [18]. Moreover, a recent study [19] tends to prove that in $PbTiO_3$ ferroelectric thin films, the polarization increases near the surface, which favours the use of negative extrapolation lengths. The best tools for detecting the surface polarization modes are probably optical techniques, like attenuated total-reflection or Raman scattering measurements. Indirect information on surface polarization modes could come from their coupling to the acoustic surface modes that could be studied using Brillouin scattering spectroscopy.

Acknowledgments

One of the authors (VD) thanks Paris-Nord University for providing a stay in the Laboratoire PMTM during which a part of this work was done.

References

[1] Paz de Araujo C, Scott J F and Taylor G W (ed) 1996 *Ferroelectric Thin Films: Synthesis and Basic Properties (Ferroelectricity and Related Phenomena vol 10)* (London: Gordon and Breach)
[2] Vinogradov E A 1992 *Phys. Rep.* **217** 159
[3] Fuchs R and Kliewer K L 1965 *Phys. Rev.* **140** A2076
[4] Mills D L and Maradudin A A 1973 *Phys. Rev. Lett.* **31** 372
[5] Fischer B and Lagois J 1979 *Excitons (Springer Topics in Current Physics vol 14)* ed K Cho (New York: Springer) p 183
[6] Jones W E and Fuchs R 1971 *Phys. Rev.* B **4** 3581
[7] Bryksin V V and Firsov Yu A 1972 *Fiz. Tverd. Tela* **14** 1148 (Engl. transl. 1972 *Sov. Phys.–Solid State* **14** 981)
[8] Tong S Y and Maradudin A A 1969 *Phys. Rev.* **181** 1318
[9] Bryksin V V, Mirlin D A and Firsov Yu A 1974 *Usp. Fiz. Nauk* **113** 29 (Engl. transl. 1974 *Sov. Phys.–Usp.***17** 305)
[10] Rimbey P R 1977 *Phys. Rev.* B **15** 1215
[11] Agarwal G S, Pattanayak D A and Wolf E 1971 *Phys. Rev. Lett.* **27** 1022
[12] Maradudin A A and Mills D L 1973 *Phys. Rev.* B **7** 2787
[13] Hopfield J J and Thomas D G 1963 *Phys. Rev.* **132** 563
[14] Cottam M G, Tilley D R and Zeks B 1984 *J. Phys. C: Solid State Phys.* **17** 1793
[15] Zhong W L, Wang Y G, Zhang P L and Qu B D 1994 *Phys. Rev.* B **50** 698
[16] Moch P, Jardin J P and Dvorák V 2000 *Ferroelectrics* **241** 141
[17] Kretschmer R and Binder K 1979 *Phys. Rev.* B **20** 1065
[18] Liu L G 1986 *J. Chem. Phys. Solids* **47** 1067
[19] Rabe K M and Ghosez P 2000 *Appl. Phys. Lett.* **76** 2767